# Chapter 32
# Carbon Nanotubes-Based Anticancer Nanomedicine

**Sougata Ghosh, Ratnakar Mishra, Amrendra K. Ajay, Nanasaheb Thorat, and Ebrahim Mostafavi**

## 1 Introduction

Cancer has emerged as the key factor for global mortality that has become a significant obstacle to life expectancy. According to World Health Organization (WHO) in 2019, maximum cancer-associated death before the age of 70 years has been reported in 112 of 183 countries. An estimated 19.3 million new cancer cases and almost 10.0 million cancer deaths occurred in 2020 globally. The most common type of cancer is female breast cancer (11.7%), followed by lung (11.4%), colorectal (10.0%), prostate (7.3%), and stomach (5.6%) cancers.

Other cancer types include various organs such as lip, oral cavity, salivary glands, oropharynx, nasopharynx, hypopharynx, esophagus, stomach, colon, rectum, anus,

S. Ghosh (✉)
Department of Microbiology, School of Science, RK University, Rajkot 360020, Gujarat, India
e-mail: ghoshsibb@gmail.com

R. Mishra
Cambridge Centre for Brain Repair and MRC Mitochondrial Biology Unit, Department of Clinical Neurosciences, University of Cambridge, Cambridge CB2 0PY, UK

A. K. Ajay (✉)
Brigham and Women's Hospital, Harvard Center for Polycystic Kidney Disease Research and Renal Division, Harvard Medical School, Boston, MA, USA
e-mail: akajay@bwh.harvard.edu

N. Thorat
Nuffield Department of Women's & Reproductive Health, Division of Medical Sciences, John Radcliffe Hospital, University of Oxford, Oxford OX3 9DU, UK

E. Mostafavi
Stanford Cardiovascular Institute, Stanford University School of Medicine, Stanford, CA, USA

Department of Medicine, Stanford University School of Medicine, Stanford, CA, USA

liver, including intrahepatic bile ducts, gallbladder, pancreas, and larynx [1]. Conventional cancer treatment includes various anticancer agents such as doxorubicin, daunorubicin, cytarabine, paclitaxel, and vincristine. However, they have potential side effects that include hypersensitivity, severe myelosuppression, nausea, neutropenia, stomatitis, rash, mucositis, vomiting, anorexia, and diarrhea [2]. Hence, it is necessary to develop innovative strategies for cancer treatment with minimum or no side effects and maximum efficacy.

Nanotechnology-driven solutions employing exotic nanostructures with notable physicochemical and opto-electronic properties have come up as an attractive alternative for cancer management [3–5]. Several metallic nanoparticles composed of gold, silver, copper, platinum, and palladium are reported to significantly inhibit the cancer cells [6–9]. Likewise, magnetic nanoparticles help in targeted delivery of drugs that avoids nonspecific drug accumulation and adverse effects [10]. The smaller dimension and the large surface area of the nanoparticles make them ideal for multifunctionalization of drugs, antibodies, peptides, nucleic acids, fluorophores, and contrast agents. Further, functionalized nanoparticles may help for tissue specific delivery of drugs, triggered release, bioimaging, and monitoring the disease progression and drug efficacy [11–13].

Carbon-based nanoparticles, particularly carbon nanotubes (CNTs) with higher penetrability, enhanced stability, and larger surface loading capacity, are considered ideal theranostic agents for their promising applications in multimodal therapy and diagnosis [14].

In this chapter, various single- and multiwalled carbon nanotubes (SWCNTs and MWCNTs)-based anticancer agents are discussed with their application in photothermal, photodynamic, chemo-photothermal, immune-photothermal, sonodynamic, and chemo-sonodynamic therapy against various cancers.

## 2  Therapeutic Modality-Based Nanomedicine

Notably, unique physicochemical and opto-electronic properties of CNTs have made them attractive nanocarriers for various drugs, targeting ligands, contrast agents for simultaneous therapy and diagnosis in cancer. Hence, CNTs-based theranostics with high capacity of binding to a wide range of biomolecules are specific to various therapeutic modalities which are discussed in detail in this section and summarized in Table 1.

### 2.1  *Photothermal Therapy*

The conventional cancer treatment strategies include chemotherapy, radiotherapy, or targeted therapies which have their own limitations due to severe non-specific adverse effects. Certain nanomaterials can convert wear near-infrared (NIR) light

**Table 1** Functionalized CNTs with various therapeutic modalities against cancer

| Sr. No. | Therapy | Nanoparticles | Functionalized ligand | Type of cancer | References |
|---------|---------|---------------|----------------------|----------------|------------|
| 1 | Photothermal | SWCNTs | Imaging agent CY7, anti-IGF-1R antibody (IGF-1R Ab) | Pancreatic cancer | [17] |
| 2 | Photothermal | SWCNTs | Annexin V | Bladder cancer | [22] |
| 3 | Plasmonic photothermal | MWCNTs | AgNPs | Melanoma | [23] |
| 4 | Photothermal | MWCNTs | Polyethylene glycol (PEG) | Melanoma | [24] |
| 5 | Photothermal | MWCNTs | Polyethylene glycol$_{5000}$ terminated with a methoxy group (DSPE–PEG), maleimide (DSPE–PEG–Mal), and fluorescein isothiocyanate (DSPE–PEG–FITC), anti-Pgp antibody | Mouse fibroblast cell line (3T3-MDR1 cells) | [25] |
| 6 | Photodynamic | (6,4)-SWCNTs | Apolipoprotein A-I (apoA-I) | Cervical cancer cells (HeLa) | [27] |
| 7 | Photodynamic | SWCNTs | Zinc mono carboxy phenoxy phthalocyanine (ZnMCPPc) and spermine | Breast cancer cells (MCF-7) | [28] |
| 8 | Photodynamic | SWCNTs | Zinc mono carboxy phenoxy phthalocyanine (ZnMCPPc) and ascorbic acid | Breast cancer cells (MCF-7) | [29] |
| 9 | Photodynamic | SWCNTs | Hyaluronic acid (HA) and chlorin e6 (Ce6) | Colon cancer cells (Caco-2) | [30] |
| 10 | Combined phototherapy | Carbon–silica nanocomposite (CSN) | D-α-tocopherol polyethylene glycol | 4T1 tumor model, patient-derived xenograft (PDX) tumor model | [33] |

(continued)

**Table 1** (continued)

| Sr. No. | Therapy | Nanoparticles | Functionalized ligand | Type of cancer | References |
|---|---|---|---|---|---|
| 11 | Combined phototherapy | SWCNTs-PEG-Fe$_3$O$_4$@CQDs | sgc8c aptamer and doxorubicin | HeLa cells and HeLa tumor-bearing nude mice | [34] |
| 12 | Chemo-photothermal | SWCNTs | Phosphatidylcholine, polyvinylpyrrolidone and curcumin | Human prostate cancer PC-3 cells and S180 tumor model in mice | [35] |
| 13 | Chemo-photothermal | MWCNTs | Lentinan, tamoxifen | Breast cancer MCF-7 cells | [36] |
| 14 | Chemo-photothermal | MWCNTs | Gemcitabine, lentinan | Breast cancer MCF-7 cells, Mcf-7 tumor-bearing BALB/c nude mice | [37] |
| 15 | Chemo-photothermal | MWCNTs | Metformin | HepG-2 cells | [38] |
| 16 | Immune-photothermal therapy | SWCNTs | Glycated chitosan | Mouse mammary tumor cell line EMT6, and mouse macrophage cell line RAW264.7, mouse mammary tumor model developed with EMT6 cells in BALB/c female mice | [39] |
| 17 | Immune-photothermal therapy | SWCNTs | Polyethylene glycol (PEG)-grafted amphiphilic polymer, combination with anticytotoxic T lymphocyte antigen-4 (CTLA-4) antibody therapy | BALB/c mice-derived dendritic cells, subcutaneous 4T1 murine breast tumors, murine B16 musculus skin melanoma | [40] |
| 18 | Immune-photothermal therapy | MWCNTs | Trastuzumab, diphtheria toxin | SK-BR-3 cells | [41] |

(continued)

**Table 1** (continued)

| Sr. No. | Therapy | Nanoparticles | Functionalized ligand | Type of cancer | References |
|---------|---------|---------------|-----------------------|----------------|------------|
| 19 | Sonodynamic therapy | MWCNTs | Polypyrrole | C540 (B16/F10) cell line and a melanoma tumor model in male BALB/c mice | [42] |
| 20 | Sonodynamic therapy | SWCNTs | Polyethylene glycol | Sarcoma 180 cells, solid tumor in CDF1 mice | [43] |
| 21 | Sonodynamic therapy | SWCNTs | Porphyrin | Human colorectal cancer cell line (HT-29) | [44] |
| 22 | Chemo-sonodynamic therapy | MWCNTs | Protohemin | HepG-2 cells, tumor in nude BALB/c mice | [45] |
| 23 | Chemo-sonodynamic therapy | MWCNTs | Folic acid, protohemin | HepG-2 cells, tumor in nude BALB/c mice | [46] |

to high heat resulting in photothermal therapy (PTT) that is able to cause mitochondrial dysfunction, generation of reactive oxygen species (ROS), and eventually cytotoxicity to cells either by apoptosis or necrosis [15]. Although various nanomaterials are fabricated for cancer treatment, they have exhibited unsatisfactory performance toward ideal PTT. Hence, carbon-based nanomaterials with unique advantages for PTT have received wide attention for their applications in biomedical field, most notable being cancer therapy. The ultrahigh specific surface area, high thermal stability, photothermal conversion efficiency, photoacoustic imaging potential, and reduced toxicity make the SWCNTs candidate photothermal agents [16].

Lu et al. reported SWCNTs-based nanoprobes coupled with the sensitive imaging agent and targeting antibodies as shown in Fig. 1 [17]. Initially, the water solubility of the raw single-walled carbon nanotubes (SWNT-RAW) was enhanced by converting them into carboxylated single-walled carbon nanotubes (SWNT-COOH) after refluxing in concentrated acid. The amphiphilic molecule, 1,2-distearoyl-sn-glycerol-3-phosphoethanolamine-N-[amino(polyethylene glycol)-5000] (DSPE-PEG5000-NH2) was attached to SWNTs by non-covalent interaction. Next, the SWNTs conjugated with DSPE-PEG5000-NH2 (SWNT-PEG) were reacted with Cyanine7-N-hydroxy-succinimide (CY7-NHS) to obtain SWNT-CY7 that attributed to its imaging property in the NIR region that directs PTT. It is important to note that the overexpression of insulin-like growth factor receptor (IGFR) in aggressive pancreatic cancer cells is associated with its proliferation, differentiation, survival, metastasis, and resistance to anticancer therapies. Hence, insulin-like growth factor type-1 receptor (IGF-1R) is considered as potential target for cancer therapy. Thus, SWNT-CY7 was further coupled with anti-IGF-1R antibody (IGF-1R Ab) to develop SWNT-CY7-IGF-1Ra so that the nanocomposite can reach the tumor via the enhanced permeability and retention (EPR) effect and simultaneously aggregate into the tumor region via antibody targeting. Substantial uptake of the nanotubes conjugated with IGF-1R Ab was observed in pancreatic cancer (BXPC-3 and PANC-1) cells. The accumulation of the nanoprobes (SWNT-CY7-IGF1-Ra) was highest at 18–24 h selectively in the tumor tissue of tumor-bearing mice which were later metabolized by the liver and intestine mainly. Laser irradiation (785 nm, 1 W/cm$^{-2}$) for 5 min significantly elevated the tumor temperature up to $48.53 \pm 1.38$ °C when treated with SWNT-CY7-IGF-1Ra resulting in marked cell damage associated with coagulative necrosis, pyknosis, apoptosis, and loss of adhesion.

Further, SWNT-CY7-IGF1-Ra mediated PTT effect in the orthotopic pancreatic cancer models exhibited high survival rate. This might be attributed to satisfactory pancreatic cancer ablation due to active targeting associated enhanced accumulation of nanotubes in the tumor tissue followed by laser treatment. In view of the background, SWNT-CY7-IGF-1Ra can be promising nanomedicine for imaging-guided photothermal therapy against pancreatic cancer.

In some cases, hyperthermia resistive tumors cannot be eradicated by slow heating from 39 °C–45 °C. In such cases, photothermal ablation is more effective as it uses light to increase the temperature within the biologic tissue above 60 °C within a short time. Due to high heat generation, death of cancerous tissue occurs via necrosis which can be a promising alternative for controlling chemoresistive as well as hyperthermic
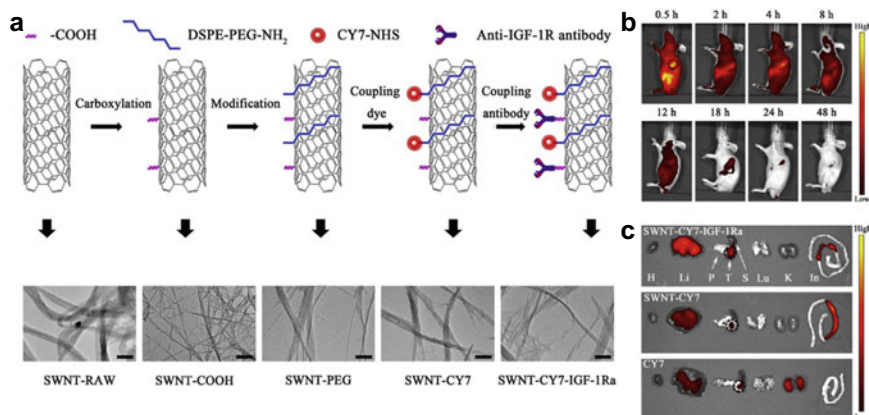
**Fig. 1** Synthesis and characterization of nanotubes. **a** Schematic illustration and TEM images in the synthesis procedure of nanotubes. The bar is 100 nm; **b** Distribution of nanoprobes in vivo. In vivo continuous observations (48 h) of mice administered SWNT-CY7-IGF-1Ra via the tail vein. The black dotted circle represents the location of the pancreatic carcinoma in situ; **c** Ex vivo imaging of tumor and major organs. **Note**: *H* heart. *Li* liver. *P* pancreas. *T* tumor. *S* spleen. *Lu* lung. *K* kidney. *In* intestine. Reprinted with permission from Lu et al. [17] Copyright 2019 Elsevier Ltd

resistive tumors [18–21]. Virani et al. reported phosphatidylserine targeted SWCNTs for photothermal ablation of bladder cancer [22]. Enhancement of nanotube accumulation inside the tumor tissue specifically was achieved by conjugating the SWCNTs with annexin V (AV), which strongly binds with phosphatidylserine (PS) present on tumor cells and tumor vasculature. Interestingly, no detectable tumor after 24 h was observed in the C57BL/6J female mice with orthotopic MB49 murine bladder tumors after treatment with the SWCNT-AV conjugate and NIR light treatment at an energy and power density of 50 J cm$^{-2}$ and 1.67Wcm$^{-2}$, respectively (time = 30 s). Rather it showed a 50% cure rate at 116 days after treatment.

Another innovative cancer treatment modality is plasmonic photothermal therapy (PPTT) where plasmonic nanoscale metals, such as silver nanoparticles (Ag NPs) with notable optical absorbance can be used in conjugation with CNTs with good thermal conductivity and cell penetration ability. Behnam et al. functionalized the MWCNTs with silver which could rapidly transform the photon energy into heat via a series of radiative and non-radiative phenomena, eventually ablating cancer [23]. The AgNPs had an average diameter of 20 nm, which were attached to MWCNTs were synthesized. Treatment with CNT/AgNPs against melanoma tumor induced by injection of B16/F10 cell line to the inbred mice exhibited enhanced optical absorption of CNTs mediated improved tumor destruction, which was attributed to PPTT brought about by irradiation via laser diode ($\lambda$ = 670 nm, $P$ = 500 mW, and $I$ = 3.5 W/cm$^2$).

Sobhani et al. improved the dispersibility of MWCNTS in water employing initial oxidation followed by surface coating with polyethylene glycol (PEG) [24]. The nanotubes with 80% PEG loading exhibited less cytotoxic activity against HeLa and

HepG-2 cell lines. On exposure to continuous-wave near-infrared laser diode ($\lambda =$ 808 nm, $P = 2$ W and $I = 8$ W/cm$^2$) for 10 min, the PEG-coated oxidized MWCNTs could sharply reduce the average size of melanoma tumor from 975 to 125 mm$^3$ in mice. Hence, such coated MWCNTs can be a powerful candidate for eradicating solid tumors employing the PTT technique.

In another study, Suo et al. proposed MWCNTs-based approach to combat P-glycoprotein (Pgp)-medicated multidrug resistance (MDR), which poses a major challenge to existing cancer therapy [25]. This novel nanocomposite was designed by combination of antibody-based cancer targeting and locoregional tumor ablation with photothermal therapy. Intercellular diffusion was enhanced, and non-specific cellular interaction was reduced using a dense coating of phospholipid−poly(ethylene glycol) around the MWCNTs. The coated MWCNTS were further chemically functionalized with an anti-Pgp antibody to facilitate Pgp-specific cellular uptake. Photothermal heating efficiency determines the toxicity of MWCNTs which generally increases with the diameter. The MWCNTs with 20–30 nm diameter generated maximum heat per unit. The MWCNTs with 8–15 nm diameter were coated with a 2 w/v % solution of a mixture of polyethylene glycol$_{5000}$ terminated with a methoxy group (DSPE–PEG), maleimide (DSPE–PEG–Mal), and fluorescein isothiocyanate (DSPE–PEG–FITC) at a 5:4:1 mass ratio followed by conjugation with Pgp antibodies (Pab) to generate Pab–MWCNTs as illustrated in Fig. 2. Acid oxidation and coating of MWCNTs using a 2 w/v % solution of DSPE–PEG reduce nonspecific cell uptake at least sixfold compared to bare MWCNTs without any loss of heat transduction capability. Moreover, this strategy dramatically increases the diffusibility of MWCNTs through the extracellular space. Cellular uptake of FITC-labeled Pab–MWCNTs was very high in the case of 3T3-MDR1 cells. The dose-dependent phototoxicity in the presence of NIR laser irradiation was notably high in Pab–MWCNTs treated 3T3-MDR1 cells. Further, the Pab–MWCNT-mediated PTT enhanced cytotoxicity against the multicellular, NCI/ADR-RES tumor spheroids which might be attributed to high intratumor diffusion and Pgp-specific cellular uptake.

## 2.2 Photodynamic Therapy

In photodynamic therapy (PDT), oxygen-dependent cytotoxicity in cancer tissue is brought about by two individually non-toxic components, one of which is a photo-sensitizer. This photosensitive molecule localizes within cancer tissue. The second component activates the photosensitizer by administering a specific wavelength of light which is followed by the generation of ROS due to the transfer of energy from light to molecular oxygen. Since this reaction is associated with the light-absorbing photosensitizer, the cytotoxicity is specific and limited to only those tissues exposed to light [26]. CNTs-based nanomedicine for PDT has become an attractive alternative cancer management strategy owing to their negligible nonspecific adverse effects.

Fukuda et al. fabricated one chiral s-SWNTs, (6,4)-SWCNTs, for photogeneration of all three major ROS, i.e., singlet oxygen ($^1O_2$), superoxide anion ($O_2^{\bullet-}$),
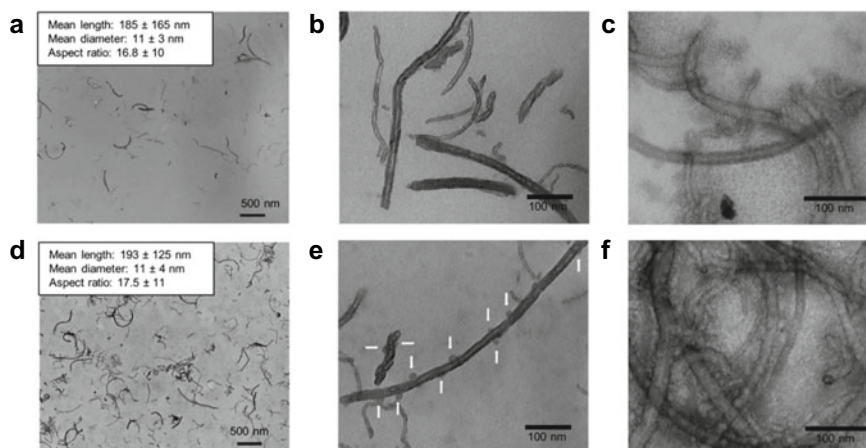
**Fig. 2** Morphological features of MWCNTs and Pab–MWCNTs. **a**, **b** Photoelectron micrographs of unstained and **c** uranyl acetate stained MWCNTs. **d**, **e** Photoelectron micrographs of unstained and **f** uranyl acetate stained Pab–MWCNTs. White arrows in **e** and globular masses (approx. 10 nm diameter) in **f** indicate the location of antibody molecules on MWCNTs. Reprinted with permission from Suo et al. [25]. Copyright 2018 American Chemical Society

and hydroxyl radical ($^{\bullet}$OH) [27]. The NIR illumination at 880 nm resulted in the photogeneration of $^{1}O_2$ by the (6,4)-SWCNTs while highly enriched (6,4)-SWCNTs resulted in abundant $^{\bullet}$OH in the presence of NIR illumination. The photodynamic effect was attributed to the intrinsic optical function of the (6,4)-SWCNTs. Further, apolipoprotein A-I (apoA-I), a lipid-binding protein of the high-density lipoprotein type, was used for functionalization where the first truncated form conjugated with the (6,4)-SWCNTs was denoted as (6,4)-SWCNTs/apo. Labeling with fluorescent Alexa Fluor 546 (Alexa546) indicated 79% accumulation of (6,4)-SWNTs/apo complexes specifically in the mitochondria, which is the predominant site of ROS generation and photodynamic therapy. Superior photostability and efficiency to generate significantly high level of $^{\bullet}$OH attributed to the enhanced photodynamic effect in (6,4)-SWCNTs. The serum protein-coated (6,4)-SWCNTs were more stable, leading to effective cancer ablation against HeLa cells where cell viability was reduced by 40%. In an interesting study, Ogbodu et al. initially conjugated zinc mono carboxy phenoxy phthalocyanine (ZnMCPPc) to spermine via amide bond which was further functionalized onto SWCNT to develop a nanocomposite denoted as ZnMCPPc-spermine-SWCNT. The loading of ZnMCPPc-spermine on SWCNTs was 42% [28]. The complex showed superior photophysical features resulting in more than 50% increase in triplet and singlet oxygen quantum yields. Photodynamic activity indicated 95% decrease in MCF-7 cell viability at 40 mM concentration with an irradiation time of 1200 s. On a similar line, ZnMCPPc was chemically modified with ascorbic acid via an ester bond to give ZnMCPPc-AA, which was further conjugated to SWCNTs via π–π interaction to give ZnMCPPc-AA-SWCNT [29]. This strategy enhanced the photophysical properties, including improved triplet lifetimes

and quantum yields and singlet oxygen quantum yields. Further, the composites showed high photodynamic activities against MCF-7 breast cancer cells with 67% decrease in cell viability. The enhanced anticancer activity might be attributed to the phthalocyanines, which are excellent photodynamic agents. Moreover, SWNTs with their photothermal properties might have enhanced the cumulative therapeutic potential. Sundaram and Abrahamse coupled SWCNTs with hyaluronic acid (HA) and chlorin e6 (Ce6) to design a nanocomposite represented as SWCNTs-HA-Ce6 [30]. The high loading efficiency of Ce6, equivalent to 70%, was attributed to the large surface area of the SWCNTs. The size and zeta potential of the nanostructure was $203 \pm 6.6$ nm and $-18.9 \pm 1$ mV, respectively. The 10 J/cm$^2$ irradiated colon cancer cells (Caco-2) showed 84.9% cell death on treatment with SWCNTs-HA-Ce6, confirming the photodynamic potential of the nanocomposite against cancer as shown in Fig. 3. Among several agents, porphyrins are the major class of photosensitizers used in photodynamic therapy, and hematoporphyrin monomethyl ether (HMME) is the newer generation of photosensitizers, which has reduced toxicity and shorter skin photosensitizing ability [31]. Photodynamic therapy of HMME combined CNTs has been shown to reduce tumor growth in mouse models [32].
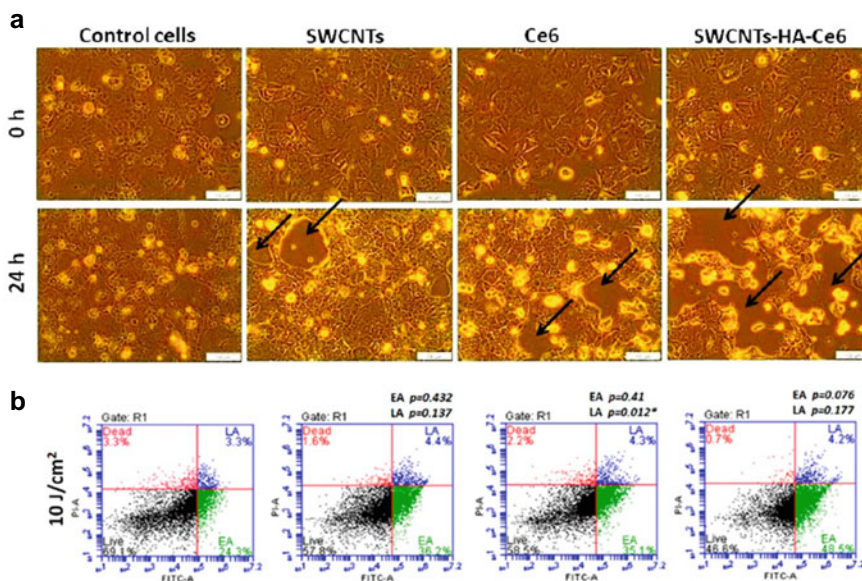


**Fig. 3** Photodynamic activity of SWCNTs-HA-Ce6 nanocomposite against colon cancer cells (Caco-2). **a** Microscopic images of untreated and treated cells (10 J/cm$^2$) of 0 and 24 h. Scale bar represents 100 $\mu$m. Black arrows indicate the cellular death. **b** Flow cytometry Annexin V PI staining analysis of apoptosis. Reprinted from Sundaram et al. [30]

## 2.3  Combined Phototherapy

Combination of phototherapy with chemotherapy or other therapeutic modalities such as radiation, chemotherapy, pre and post-surgery treatments to enhance the cancer cell killing and achieve higher therapeutic index has gained significant interest in the past few years. The development of novel nanomaterials and their combination with phototherapy provides wide range of modulating power for designing specific and controlled therapeutic methods.

Wang et al. fabricated a degradable carbon–silica nanocomposite (CSN)-based immunoadjuvant [33]. In this process, 3D dendritic degradable mesoporous silica nanoparticle (MSN) was initially synthesized using triethanolamine (TEA), cetyltrimethylammonium chloride (CTAC), tetraethyl orthosilicate (TEOS), and cyclohexane was added at 60 °C as depicted in Fig. 4. The MSN powders were finally recovered by drying at 50 °C in a vacuum. Further, the MSNs were reacted with (3-aminopropyl)triethoxysilane (APTES) for 20 h at 80 °C in order to modify the amino group on the surface of the MSNs. The NH2-MSN was reacted with α-D-glucose for 20 h at 160 °C to prepare MSN@Glu that was further dried and carbonized under a nitrogen atmosphere at 540 °C for 4 h to obtain the CSN. D-α-tocopherol polyethylene glycol was used for modifying the CSNs. Monodispersed CSN exhibited uniform particle size of 100 nm, which is advantageous for enhanced accumulation in the tumor region via enhanced permeability and retention (EPR) effect. The elemental composition of the CSN was contributed by carbon, silicon, oxygen, and nitrogen with mass percentages (wt%) of 36.1%, 27.6%, 35.0%, and 1.3%, respectively. The photothermal property was indicated by a sharp increase in temperatures (27.6–78.2 °C) of CSN dispersions under NIR light (808 nm, $2\,\mathrm{W\,cm^{-2}}$) irradiation was a function of time (10 min) and concentration ($200\,\mathrm{\mu g\,mL^{-1}}$). The photothermal conversion efficiency ($\eta$) of CSN was ∼34.5%.

Generation of singlet oxygen ($^1O_2$) by the CSN in combination with NIR increased by 124.7%, confirming its superior photodynamic property. The CSN facilitated maturation of bone marrow-derived dendritic cells (BMDCs) from BALB/c mice which was associated with higher expression of costimulatory CD80, CD86, tumor necrosis factor-alpha (TNF-α) and interleukin-6 (IL-6). It was speculated that the rough surface of CSN with 100 nm size could be efficiently taken up by the DCs followed by the maturation of DCs. The superior photothermal and photodynamic properties of the CSN were exploited for antitumor efficiency in combination with NIR light in 4T1 tumor model as shown in Fig. 5a, b. Tumor in mice was inhibited up to 93.2% on treatment with CSN with NIR. Further, patient-derived xenograft (PDX) tumor model was developed by subcutaneous injection of human CRC cancer tissue fragments into B-NDG mice. Treatment with CSN in combination with NIR exhibited 92.5% suppression of the tumor growth in PDX tumor-bearing mice as shown in Fig. 5c, d. Hence, carbon–silica-nanomaterial-based therapeutic strategy can be promising next-generation anticancer nanomedicine.

Zhang et al. reported fabrication of novel magnetofluorescent $Fe_3O_4$/carbon quantum dots (CQDs)-coated SWCNTs as trimodal therapeutic agents with imaging
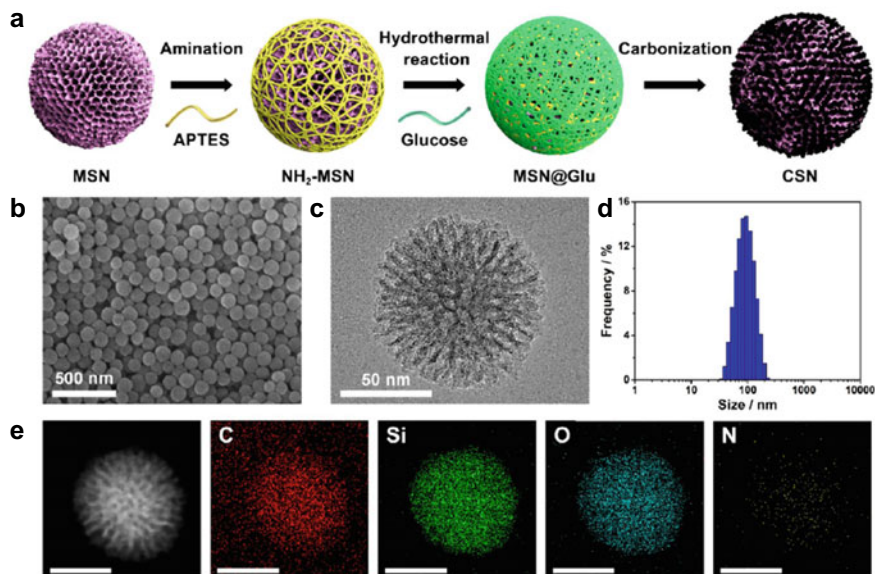
**Fig. 4** Synthesis and characterization of CSN. **a** Schematic illustration of CSN synthesis. **b** Scanning electron microscope (SEM) and **c** high-resolution transmission electron microscope (HR-TEM) images of CSN. **d** Size distribution of CSN. **e** High-angle annular dark field scanning TEM (HAADF-STEM) image and element mapping of CSN. Scale bar: 50 nm. Reprinted with permission from Wang et al. [33]. Copyright 2020 American Chemical Society
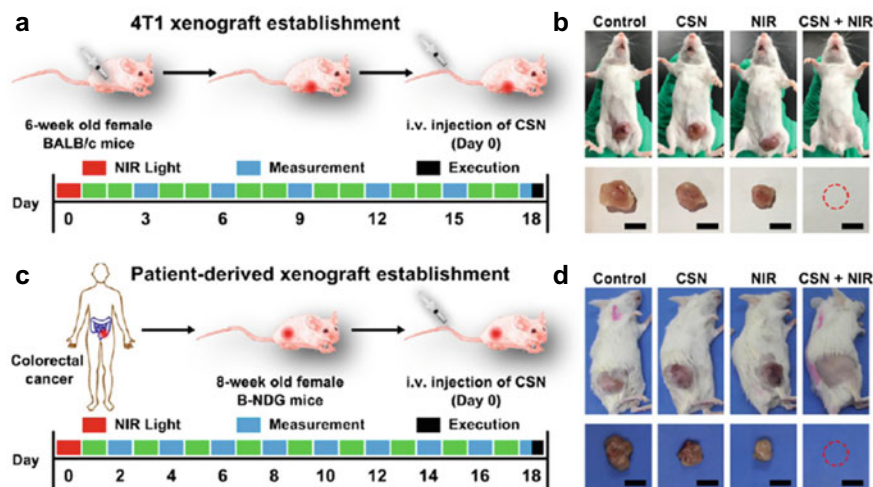


**Fig. 5** In vivo antitumor experiments of CSN. Schematic illustration of the establishment of **a** 4T1 and **c** PDX tumor models and therapy procedure of CSN (1 mg mL$^{-1}$, 200 µL) combined with NIR light (808 nm, 2 W cm$^{-2}$, 5 min) irradiation ($n = 5$). Photographs of **b** 4T1 and **d** PDX tumor-bearing mice, as well as corresponding dissected tumors after the therapy. Scale bar: 1 cm. Reprinted with permission from Wang et al. [33] Copyright 2020 American Chemical Society

as well as chemo/photodynamic/photothermal (CT/PDT/PTT) properties [34]. Initially, the branched PEG 2000 N was grafted covalently (with 17.8% loading) on the surface of oxidized and shortened SWCNTs with more carboxylic acid group on its side walls. The polymer shell was 5–7 nm thick. Hydrothermally synthesized spherical CQDs were $2.8 \pm 0.3$ nm in size. Further, doxorubicin (DOX), a standard anticancer drug, was loaded into the pore structure of the synthesized SWCNTs-PEG-$Fe_3O_4$@CQDs nanocarriers with high efficiency which were then conjugated with a sgc8c aptamer, denoted as SWCNTs-PEG-$Fe_3O_4$@CQDs-DOX-Apt, for targeting dual modalfluorescence/magnetic resonance (MR) imaging. It is important to note that the SWCNTs-PEG-$Fe_3O_4$@CQDs exhibited superior upconverted photoluminescence properties and can be excited by long-wavelength light ($\lambda > 600$ nm) with the upconverted emissions located in the range of 420–520 nm. Significant reduction in viability of HeLa cells on treatment with SWCNTs-PEG$Fe_3O_4$@CQDs was attributed to the simultaneous generation of $OH^\bullet$ and $^\bullet O_2{}^-$, DOX release and hyperthermia-associated CT, PDT, and PTT using a single NIR laser. Interestingly, Fig. 6 shows rapid increase of the temperature at the tumor site to 52 °C in the presence of SWCNTs-PEG-$Fe_3O_4$@CQDs/DOX-Apt upon NIR laser illumination (within 5 min) HeLa tumor-bearing nude mice. Due to combined therapy, the tumor volume reduced significantly.

Hence, this combined therapeutic strategy demonstrates exceptional success through irradiation to generate limited heat for cancer cell killing for more specific induction of necrosis or apoptotic cell death only in irradiated cancer cells/tissues.

## 2.4 Chemo-Photothermal Therapy

CNTs provide ideal surfaces for functionalization of chemotherapeutic agents with anticancer potential. Such nanocomposites exhibit promising chemo-photothermal properties because of their remarkable cell membrane penetrability, sustained release and noteworthy photothermal effects. In one such study, Li et al. conjugated curcumin to SWCNTs functionalized with phosphatidylcholine and polyvinylpyrrolidone to yield SWCNT-Cur [35]. Sixfold increase in the cellular uptake of SWCNTs-Cur by human prostate cancer PC-3 cells was observed. Further, the concentration of curcumin increased 18-fold in blood along with residence time on treatment with SWCNT-Cur. Synergistic tumor suppression by SWCNT-Cur in combination with 808 nm laser irradiation at 1.4 W/cm$^2$ was noticed along with reduction in tumor weight and volume in S180 mice tumor models.

In another study, a natural biological polysaccharide, lentinan (LEN), was initially functionalized on MWCNTs for delivery of an anticancer drug, tamoxifen (TAM) which is schematically represented in Fig. 7 [36]. The loading ratio of TAM and LEN in the composite (MWCNTs-TAM-LEN) was 28.6% and 26.5%, respectively. The nanocomposite not only exhibited superior stability and water dispersibility but also demonstrated remarkable photothermal properties. The MWCNTs-TAM-LEN was further labeled with Rhodamine 123 which showed enhanced cellular uptake by
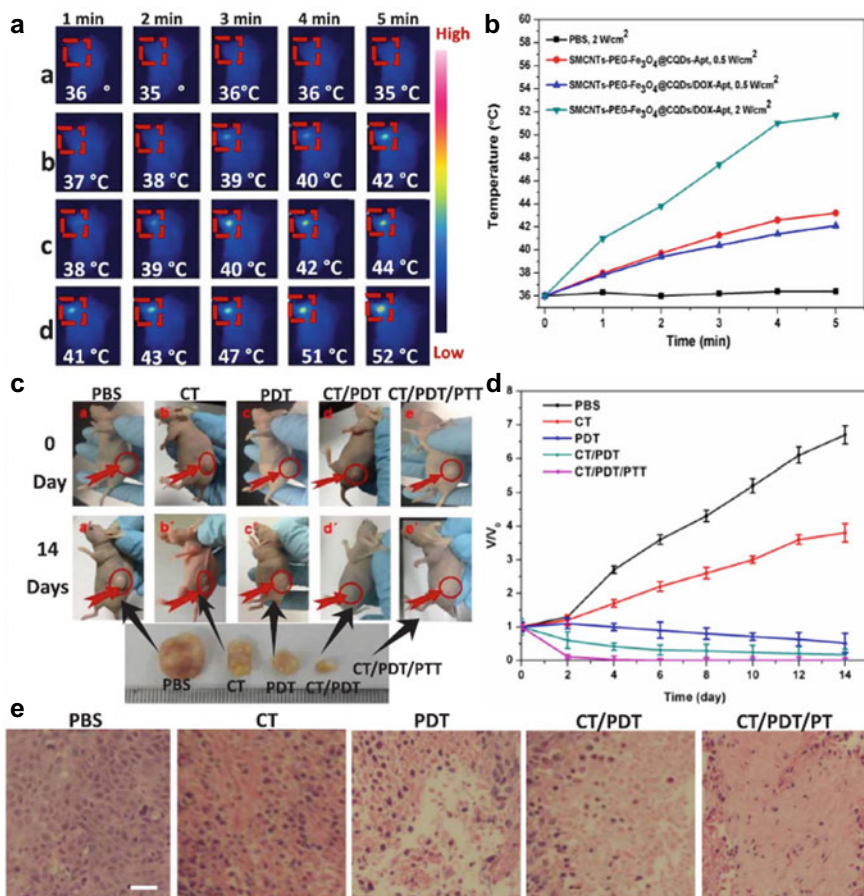
**Fig. 6** **a** IR thermal images of HeLa tumor-bearing mice incubated with various media: *a* PBS, *b* 100 µg/mL of SWCNTs-PEG-Fe$_3$O$_4$@CQDs-Apt + laser (808 nm, 0.5 W/cm$^2$), *c* 100 µg/mL of SWCNTs-PEG-Fe$_3$O$_4$@CQDs/DOX-Apt + laser (808 nm, 0.5 W/cm$^2$) and *d* 100 µg/mL of SWCNTs-PEG-Fe$_3$O$_4$@CQDs/DOX-Apt + laser (808 nm, 2 W/cm$^2$). **b** Heating curve of the five laser-irradiated groups. **c** Representative photographs of tumor-bearing mice after different treatments. **d** Time-dependent tumor growth curves observed after different treatments ($n = 5$, $P < 0.05$ for each group). **e** H&E staining of tumor sections gathered from various treatment groups of mice on day 2. Scale bar = 50 µm. Reprinted with permission from Zhang et al. [34]. Copyright 2018 Elsevier B.V.

MCF-7 cells due to penetration into the cell membrane followed by accumulation in the cytoplasm. High cell growth inhibition up to ~91.7% was observed when treated with MWCNTs-TAM-LEN in combination with NIR irradiation at the TAM concentration of 5 µg mL$^{-1}$. Similarly, rate of apoptosis increased to 78.11% when the MCF-7 cells was treated under aforementioned condition.

Zhang et al. fabricated a drug delivering three-component composite denoted as MWCNTs-Ge-Le comprised of MWCNTs, gemcitabine (Ge) and lentinan (Le) as
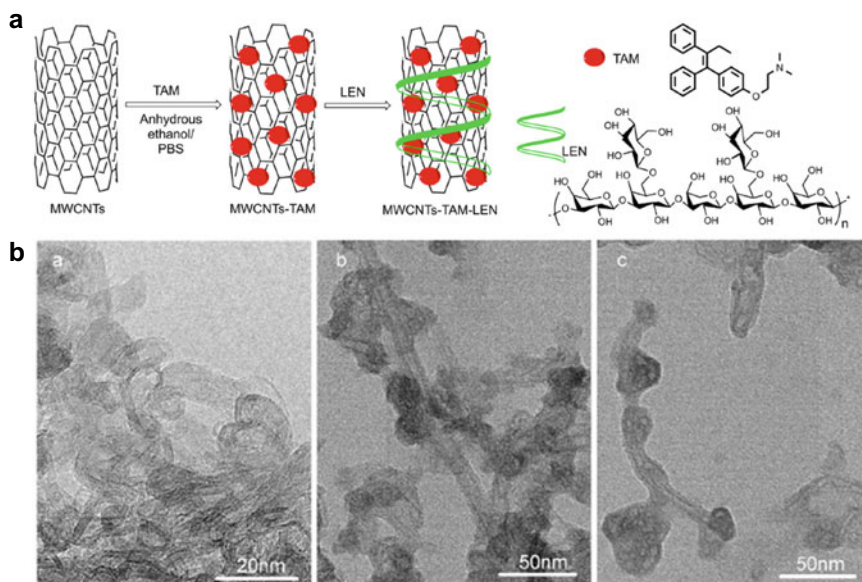
**Fig. 7** **a** Illustration diagram of MWCNTs-TAM-LEN synthesis; **b** TEM images of MWCNTs (*a*) and MWCNTs-TAM-LEN (*b* and *c*). Reprinted with permission from Yi et al. [36]. Copyright 2018 Elsevier B.V.

schematically represented in Fig. 8 [37]. The nanocomposite displayed antitumor activity which was attributed to combination of chemotherapy and photothermal therapy. Loading of gemcitabine and lentinan in MWNTs-Ge-Le was 31.8% and 10.4%, respectively. The increase in temperature from 25 to 45 °C under 2 W cm$^{-2}$ NIR irradiation for 10 min indicating its photothermal property of the MWCNTs-Ge-Le solution (25 $\mu$g mL$^{-1}$). After tagging with rhodamine 123, the MWCNTs-Ge-Le was observed to be internalized within the MCF-7 cells within 3 h followed by dose-dependent antiproliferative effects. MWCNTs-Ge-Le combined with NIR irradiation exhibited remarkable inhibitory effects on cancer cells. The temperature of tumor site increased to 42.6 °C on treatment with MWCNTs-Ge-Le in presence of 808 nm laser NIR irradiation (1 W cm$^{-2}$, 3 min). This was attributed to maximum accumulation of MWCNTs-Ge-Le nanoparticles at the tumor site through EPR effect. Hence, this synergistic strategy of combining drug therapy with near-infrared photothermal therapy can be a powerful tool for treatment and management of cancer.

In another study, Yoo et al. designed a nanocomposite (MWCNTs-Met/PEG) by functionalizing an antidiabetic drug metformin (MET) on the MWCNTs via PEGylation [38]. The nanocomposite metformin and PEG content of 22.5% and 15.7%, respectively. MWNTs-Met/PEG solution rapidly increased beyond 45 °C under 2 W cm$^{-2}$ NIR irradiation confirming the photothermal effect of the MWCNTs-Met/PEG toward induction of strong localized heating associated pro-apoptosis.
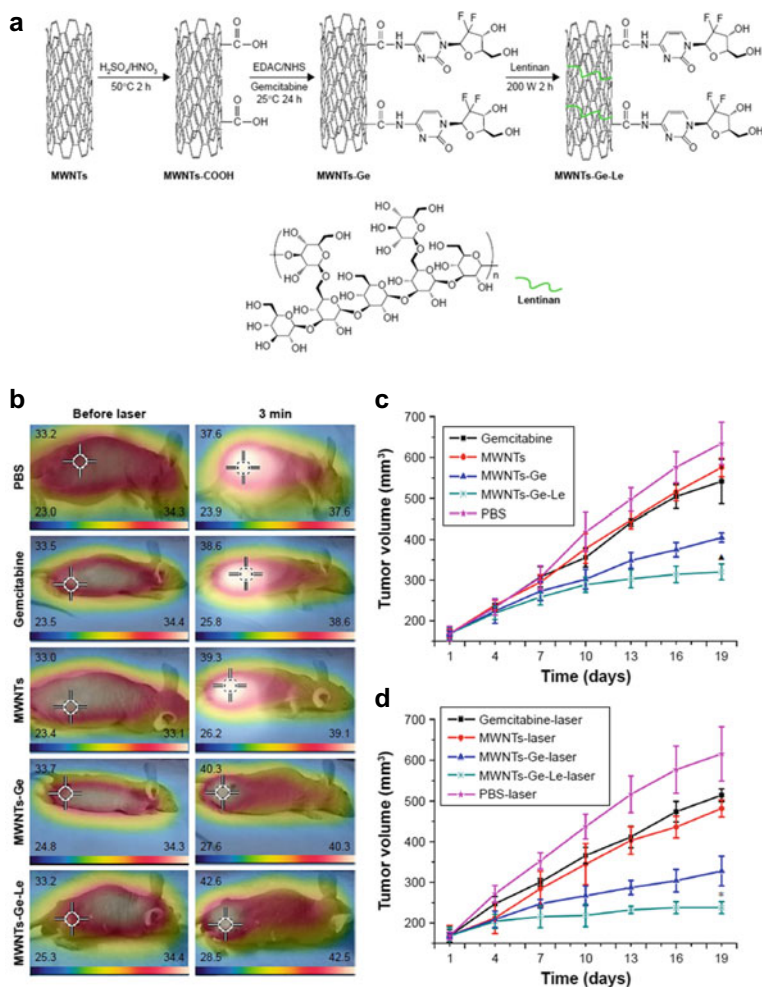
**Fig. 8 a** Approach for preparing MWNTs-Ge-Le; **b** In vivo antitumor effect. Infrared thermographic images of tumor-bearing mice after treatment with PBS, gemcitabine, MWNTs, MWNTs-Ge and MWNTs-Ge-Le followed by laser irradiation. The scale bar is different for each image; **c** Average tumor volume in a MCF-7 tumor-bearing mice model of treatment without laser in vivo; **d** Average tumor volume in a MCF-7 tumor-bearing mice model of treatment with laser in vivo. The relative tumor volumes were normalized to their initial size ($n = 4$ for each group). The bars are presented as mean $\pm$ SEM (unpaired $t$-test, *$P < 0.05$ compared with all the other experimental groups; ▲$P < 0.05$ compared with PBS group, gemcitabine group, MWNTs group and MWNTs-Ge group). **Abbreviations**: *EDAC* 1-(3-dimethylaminopropyl)-3-ethylcarbodiimide; *MWNTs* multiwalled carbon nanotubes; *MWNTs-COOH* oxidized multiwalled carbon nanotubes; *MWNTs-Ge* multiwalled carbon nanotubes/gemcitabine; *MWNTs-Ge-Le* multi-walled carbon nanotubes/gemcitabine/lentinan; *NHS N*-hydroxysulfosuccinimide; *Mcf-7* Michigan cancer foundation-7; *NIR* near-infrared; *PBS* phosphate-buffered solution; *SEM* standard error of the mean. Reprinted with permission from Zhang et al. [37] Copyright 2018 Dove Medical Press Limited

Internalization within HepG-2 cells took place in 3 h. Cell viability in the HepG-2 cells drastically fell to $5.7 \pm 1.2\%$ on treatment with MWNTs-Met/PEG in combination with NIR irradiation.


## 2.5   Immune-Photothermal Therapy

Although PTT is effective for treating cancer cells locally as they are sensitive to high temperature, weak immunogenicity of tumors is a major challenge. Hence, combination of PTT and active immunological stimulation can synergistically improve the effectiveness of the anticancer therapy. Zhou et al. designed immunologically modified SWCNTs-based system employing an immunoadjuvant, glycated chitosan (GC) denoted as SWCNTs-GC [39]. A concentration and laser dose-dependent rise in temperature from 30 to 60 °C was observed when the SWCNT-GC was irradiated with a 980 nm laser at 0.5–1 W/cm$^2$ for 120 s. SWNT-GC exhibited superior stimulation of NO production in macrophages along with expression of CD80 indicating the maturation of dendritic cells. The SWNT-GC tagged with FITC entered into EMT6 cells and accumulated in the cytoplasm. The nanocomposite also accumulated in the RAW264.7 cells owing to phagocytosis in macrophages and stimulated a higher level of IFNγ secretion. Mouse mammary tumor developed by injecting EMT6 cells in the flank of Balb/c female mice was treated with SWNT-GC in combination with laser irradiation with a power density of 0.75 W/cm$^2$ for 10 min and showed drastic elevation in the temperature. Within 2 min, the tumor tissue surface temperature rose to 62 °C that began to plateau after 5 min at 72 °C which resulted in induction of 89.2% apoptosis.

In another extensive study by Wang et al., photothermal ablation of primary tumors with SWCNTs in combination with anticytotoxic T lymphocyte antigen-4 (CTLA-4) antibody therapy was demonstrated to be highly effective against tumor metastasis in mice as schematically illustrated in Fig. 9 [40]. The SWCNTs were non-covalently modified using polyethylene glycol (PEG)-grafted amphiphilic polymer. This composite not only destroyed tumor due to photothermal properties but also triggered the release of tumor-associated antigens and served as an immunological adjuvant facilitating the maturation of bone marrow-derived dendritic cells (DCs) separated from BALB/c mice. Further, the PEGylated SWCNTs up-regulated the expression of CD86 and CD80 along with enhancement of interleukin IL-1β and IL-12 secretion by DCs. The nanomaterial treated mice bearing subcutaneous 4T1 murine breast tumors showed high tumor ablation on irradiation with an 808-nm NIR laser at 0.5 W/cm$^2$ for 10 min due to dramatic temperature elevation to 53 °C in the tumor tissues. It is important to note that this therapeutic strategy completely eliminated all tumors in mice without showing a single case of tumor relapse at their original sites after treatment. SWCNTs-based PTT mediated enhancement in the secretion of pro-inflammatory cytokines IL-1β, IL-12p70, IL-6, and TNF-α was

speculated as the key immunomodulatory effect behind the effective tumor inhibition. Additionally, anti-CTLA-4 antibody is able to target CTLA-4, which is constitutively expressed by regulatory T cells (Tregs) and up-regulated after T cell activation. Hence, SWNT-based PTT-associated CTLA-4 blockade may favor the infiltration of effective T cells while greatly abrogate regulatory T cells at distant tumors. The study showed that primary tumor ablation employing SWNT-based PTT followed by CTLA-4 blockage significantly inhibited the development of secondary tumors. This might be attributed to the CD8$^+$ killer T cells [cytotoxic T (Tc) cells] mediated destruction of cancer cells by releasing cytotoxins perforin, granzymes, and granulysin that eventually result in apoptosis of targeted cancer cells. Moreover, a combination of SWNT-based PTT and anti-CTLA-4 therapy significantly reduced lung metastasis with less than 1 metastasis sites in lungs. Additional study in murine B16 musculus skin melanoma indicated that residues of both 4T1 cells and B16 cells after SWCNT-based PTT activated DC maturation.

In an innovative research, Kohshour et al. exploited trastuzumab (Herceptin®), a monoclonal antibody (mAb) for specific ablation of malignant breast cancer cells that over-expressed HER2 [41]. Proliferation of the cancer cells was effectively inhibited by MWCNTs-based nanoimmunoconjugate comprised of covalently immobilized trastuzumab conjugated to diphtheria toxin (DT). The cell viability of HER2-overexpressing SK-BR-3 cells was reduced to 70.42% and 80% by trastuzumab-MWCNT conjugates and trastuzumab-DT, respectively.
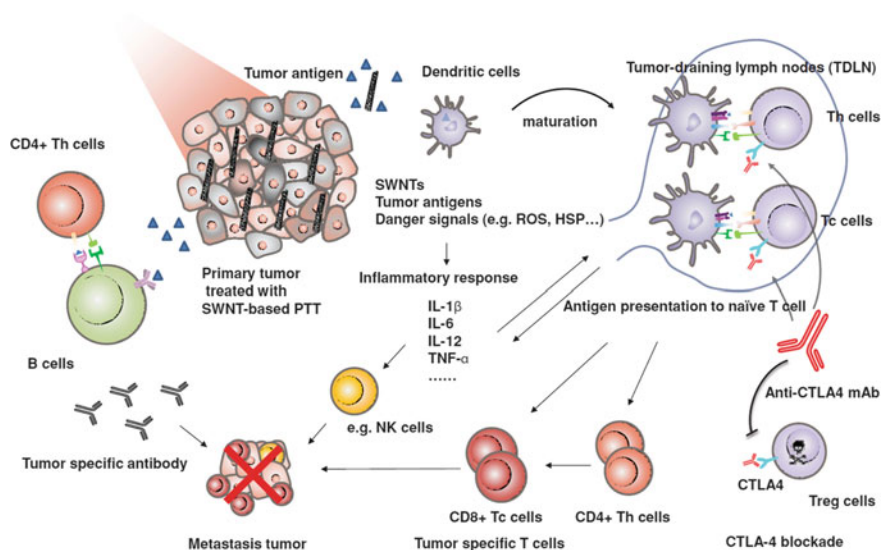


**Fig. 9** Hypothesized mechanism of antitumor immune responses induced by SWNT-based PTT in combination with the anti-CTLA-4 therapy. Reprinted with permission from Wang et al. [40] Copyright 2014 WILEY–VCH Verlag GmbH & Co. KGaA, Weinheim

## 2.6  Sonodynamic Therapy

Sonodynamic therapy (SDT) has come up as an innovative and effective strategy for treating solid cancers employing ultrasound irradiation of low-intensity along with a sonosensitizer. This therapeutic mode is advantageous due to its very low or negligible adverse effects and invasiveness, deep tissue penetration, and targeted uptake. Behzadpour et al. fabricated a polypyrrole-coated MWCNTs-based nanocomposite (PPy@MWCNTs) which exhibited superior sonosensitizing properties due to its efficient absorption of ultrasound irradiation by both of its components [42]. The PPy@MWCNTs were comprised nanotubes with $36.3 \pm 5.1$ nm of diameter and several micrometer in length. Ultrasound irradiation at 1 MHz and 1.0 W cm$^{-2}$ for 60 s resulted in rise in $16.3 \pm 2.8$ °C increment in temperature. The nanocomposite exhibited a concentration-dependent cytotoxicity on multistep ultrasound irradiation against C540 (B16/F10) cell line and a melanoma tumor model in male balb/c mice. After ten days of SDT using PPy@MWCNTs, 75% necrosis was observed in the tumors that led to 50% decrement in tumor volume. The higher antitumorigenic properties could be attributed to the cumulative thermal effects and ROS generated during the PPy@MWCNTs-associated SDT.

In another study, Yumita et al. reported SDT using polyethylene glycol-modified carbon nanotubes (PEG-modified CNTs) [43]. Sonodynamic exposure to PEG-modified CNTs resulted in twofold cytotoxicity in sarcoma 180 cells which was attributed to the singlet oxygen generated during the treatment. Further, 100 μM PEG-modified CNTs enhanced the nitroxide production up to threefold. Combination of ultrasound and PEG-modified CNTs synergistically inhibited the solid tumor growth in CDF1 mice with the carcinoma cells transplanted subcutaneously in the left dorsal scapula region. In a similar work, Bosca et al. fabricated a porphyrin grafted SWCNTs for SDT where three different porphyrins were covalently conjugated to SWCNTs using either Diels–Alder or 1,3-dipolar cycloadditions [44]. ROS production was enhanced and cell viability of the human colorectal cancer cell line (HT-29) significantly reduced upon ultrasound irradiation in spite of low porphyrin content indicating the efficiency of the therapy.

## 2.7  Chemo-Sonodynamic Therapy

Occassionally ultrasound-based SDT employ a sonosensitizer in combination with a chemotherapeutic agent which is referred as chemo-sonodynamic therapy. This strategy is more effective for treating cancer by induction of apoptosis and/or necrosis. Wang and Li encapsulated a sonosensitizer, protohemin (Ph) non-covalently into MWCNTs-COOH (MWCNTs-Ph) enhanced antitumor efficiency [45]. About 68.8% (w/w) Ph loading was achieved on MWCNTs-COOH carrier. In presence of ultrasound (1.0 MHz and 0.5 W/cm$^2$ for 100 s), MWCNTs-Ph remarkably inhibited the growth of HepG-2 cells up to $95 \pm 8.5\%$. Tumor developed in mice

by subcutaneous injection of HepG-2 cells into the right armpit of nude BALB/c mice was inhibited more than 80% on treatment with MWCNTs-Ph and ultrasound together. Hence, MWCNTs-Ph-based cancer management can serve dual purpose of tumor inhibition and reduction of side effects. On a similar line, Wang et al. covalently attached oridonin-liposome containing microbubbles (LUMO) to folic acid-conjugated MWCNTs functionalized with protohemin (FMTP) to form a novel composite (FMTP-LUMO) [46]. Oridonin used in this composite is a chemotherapeutic drug for chemotherapy, whereas protohemin is a sonosensitizer as stated previously. In combination with ultrasound, the FMTP-LUMO inhibited the HepG-2 cells up to $95.4 \pm 5.9\%$ which might be attributed to superior release profile (90%) of oridonin due to ultrasound exposure of 60 s. Further, FMTP-LUMO treated liver cancer induced by implantation of HepG-2 cells in BALB/c nude mice showed more than 90% tumor inhibition after ten days.

## 3 CNTs-Based Strategies Against Nervous System-Associated Cancer

Developing CNTs-based nanomedicine against cancer of the brain is one of the most challenging tasks which need thorough understanding about the physiological, biochemical, immunological, and genetic attributes of the cancer. The growing cancer cells generate a lot of pressure inside the skull and could be life-threatening. Cancer-associated uncontrolled cell growth in the brain forms a tumor-like mass in most cases and is commonly referred to as a brain tumor. A brain tumor is classified into two different classes based on its point of origin—primary and secondary type of brain tumor. Primary brain tumor originates in the brain itself while in the secondary brain, tumor metastasizes from another organ to the brain [47]. The primary brain tumor generally originates from glial cells and is referred to as glioma. There are four different grades of glioma based on size and growth (grade I–IV), grade I glioma does not infiltrate deep into the brain tissue and could be treated by surgical interventions, whereas grade IV glioma infiltrates deep into the brain tissue, called as glioblastoma are difficult for surgical interventions [48]. Stage IV glioblastoma is the most common type of brain cancer with 17,000 new diagnoses every year and is associated with a median survival rate of 14 months with poor life quality [48, 49].

Currently, there is no complete cure for glioblastoma and the patients generally survive for less than two years [50–53]. The current treatment strategy includes the use of aggressive anticancer drugs, surgery, radiation, and chemotherapy [53–55]. Such aggressive treatment has a lot of side effects and with high chances of tumor recurrence; the patients typically die within two years of treatment. The treatment of glioblastoma is difficult even with radiation and chemotherapy due to the highly invasive nature of the brain tumor; thus, a targeted drug delivery system could be used for delivering anticancer or immunotherapeutic drugs [53].

CNTs are biocompatible, hollow, tubular nanostructures that have extensive therapeutic potential as a drug delivery system, imaging tool, and implantable devices in the nervous system as well [56]. The reason for the low success rate of brain tumor treatment lies mainly with the invasive nature of the tumor, and the penetration of the treatment molecule through the blood–brain barrier (BBB). The tumor is formed deep inside the brain tissue which is difficult to access by surgery or with radiation; therefore, a perfect drug delivery system is required to direct the therapeutic molecules to the brain tumor and cross the BBB. The latest understanding of molecular details and cellular pathways of glioblastoma is paving way for use of SWCNTs and MWCNTs for the treatment of brain gliomas due to their length/diameter ratio, electrical conductivity, biological compatibility, and easy conjugation with therapeutic or diagnostic molecules [53, 54, 57, 58].

One of the limiting factors in the treatment of glioblastoma is the migration or invasiveness of the tumor cells deep into the brain tissue. In a study, Alizadeh and colleagues demonstrated that CpG oligodeoxynucleotide (CpG ODN) bound with CNTs inhibits the migration of the glioblastoma cells via activating toll-like receptor 9 [53]. CpG ODN is a synthetic single-stranded DNA molecule that contains unmethylated cytosine and guanine motifs derived from bacterial DNA. Therapeutic mechanism of CpG ODN includes protective immunity, cancer therapy, increasing the response to the vaccine, and suppression of allergic reactions [59, 60]. Hence, the use of CpG with suitable CNTs can have multiple therapeutic potentials in cancer therapy as well as in modulating the immune response of the body as illustrated in Fig. 10.

SWCNTs conjugated with CpG (SWCNTs/CpG) showed greater immunostimulatory effects than compared to free CpG in glioma models [61, 62]. A single dose of intracranial injection of SWCNTs /CpG in a GL261 murine model eradicated the gliomas in 50–60% of the mice, suggesting the high efficacy of SWCNTs/CpG in cancer treatment [61]. Furthermore, the glioblastoma chemotherapy drug molecule temozolomide showed enhanced effect when combined with SWCNTs/CpG in the treatment of the glioma mouse model [62]. The in vitro glioma histology suggests that SWCNTs/CpG locally alters the invasive properties of the tumor by inhibiting the migration of glioma cells followed by decreased NF-κB activation and an overall reduction in intracellular ROS [53]. Thus, SWCNTs/CpG could be tested in future clinical trials for the treatment of glioblastoma due to its ability to activate the innate immune system and inhibit the migration of tumor cells to the brain tissue (migration of tumor cells is one of the most challenging aspects in treating glioblastoma.

Another limiting aspect of brain tumor treatment is the delivery of therapeutic molecules across the blood–brain barrier (BBB) to the glioma [63]. BBB is a highly selective semipermeable membrane covering the central nervous system, made of tightly packed endothelial cells which prevent the passage of blood-borne pathogens and non-selective molecules from the circulating blood into the cerebrospinal fluid of the central nervous system [64]. In a study, MWCNTs conjugated with $NH_3^+$ were able to cross BBB in an in vitro model of BBB composed of porcine brain endothelial cells and rat primary astrocytes cells [65]. In cancer treatment, MWCNTs conjugated with cell-penetrating peptide (CPP) and anticancer molecule showed
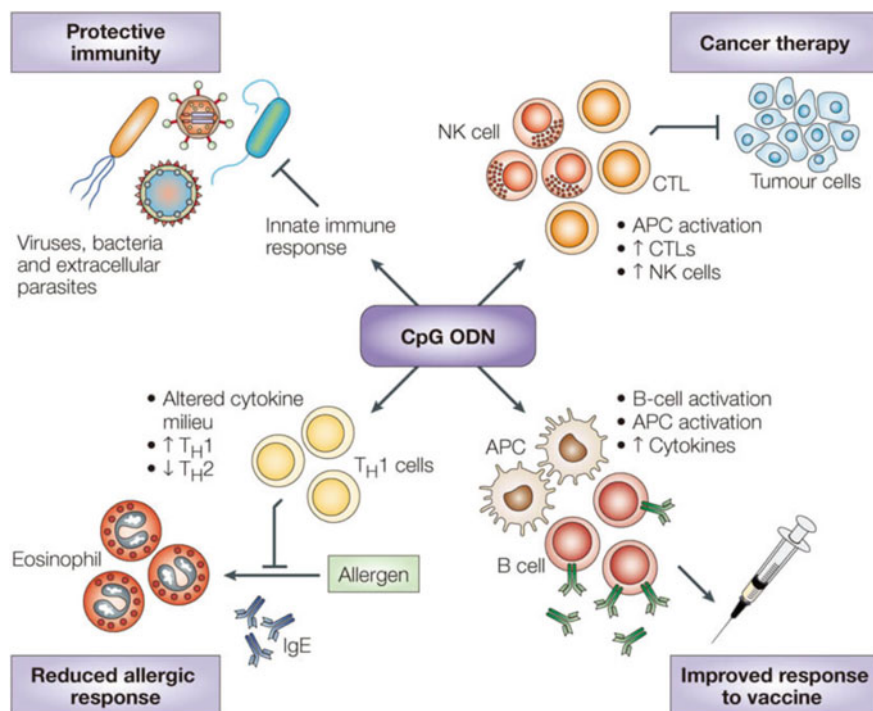
**Fig. 10** Proposed therapeutic application of CpG based on the interaction of CpG with cells of the immune system. Reprinted with permission from Klinman [59]. Copyright 2004 Nature Publishing Group

enhanced BBB penetration and anticancer activity for glioma treatment [63]. CPP like trans-activating transcriptional activator (TAT) was used in the previous study to increase the permeability of BBB [66]. However, increasing the permeability also increases the chances of non-specific penetration of CPP [67]. You and colleagues have designed and synthesized MWCNTs loaded with TAT and anticancer drug oxaliplatin for the precise targeting of glioma. The results of this study suggest that the MWCNTs with TAT and oxaliplatin were more cytotoxic to the glioma cells compared to free oxaliplatin [63]. Thus, SWCNT and MWCNT could be effectively be used as drug delivery machinery which could cross the BBB and specifically target the brain tumor cells inhibiting its further migration into the deep brain tissue. However, more detailed studies are required to completely establish the molecular mechanism of CNTs interactions in brain tumor treatment before it could be tested in clinical trials. Figure 11 summarizes the key points that could be achieved by the use of CNTs in brain cancer treatment.

The brain is not the only organ of the nervous system that is affected by cancer; the cancer of the retina called retinoblastoma, is one of the most common types of intraocular cancer mostly affecting young children [68, 69]. The most common symptom of
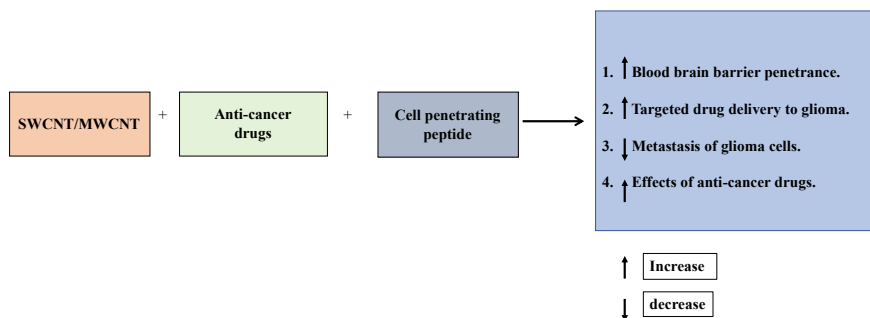
**Fig. 11**  Therapeutic potential of CNTs in brain tumor treatment

retinoblastoma is visible whiteness in the pupil of the eye called Leukocoria, notice-able in dim light [70]. Retinoblastoma is highly sensitive to chemotherapy treatment and can be treated by injecting chemotherapy drugs either directly in the ocular cavity or intravenously [68]. The use of CNTs in retinoblastoma treatment can further enhance the uptake of chemotherapy drugs during the treatment. The retinoblastoma cells have a high affinity for folic acid and biotin because of the enrichment of folate and biotin receptors on retinoblastoma cells [71–73]. Demirci and colleagues had demonstrated that CNTs conjugated with fluorescein isothiocyanate and folic acid/ biotin (CNTs-FITC-FA/Bio) injected into the vitreous humor of the transgenic retinoblastoma mice model show high penetration into the retinoblastoma cells [74]. In view of the background, CNTs-FITC-FA/Bio composite can serve as a promising drug delivery system for the delivery of chemotherapeutic agents for treatment of intraocular tumors [74]. The studies so far suggest the potential application of CNTs in the treatment of cancers of the nervous system. However, the details regarding the cytotoxicity and uptake of CNTs by the nervous system are not completely under-stood, which is one of the limiting factors for potential use of CNTs for treating nervous system-associated cancers.

## 4   Future Perspectives

Development of cancer drug resistance is major challenge for the existing chemother-apeutic strategy. Hence, nanotechnology-driven solutions are thought to be better candidates with multimodal therapeutic perspectives. Cancer therapy combining chemoradiation with sonodynamic therapy has been shown to decrease tumor growth in pancreatic cancer cellular models [75]. Gold nanoparticles release heat through a light-driven surface plasmonic process [76–78]. Similarly, conjugation of organic polymer particles has shown high heat transfer efficiencies [79–81]. Hence, getting synergistic efficacy by combinatorial approaches has been a topic of research to enhance cancer therapeutic efficacy. Combination of chemotherapeutic drugs with

CNTs-associated photothermal treatments can show promising for various cancer treatments that can be confirmed using cell-based in vitro studies and in mouse models. Photothermal treatment employing CNTs combined with daunorubicin and cytarabine may promote cell apoptosis [82]. Likewise, doxorubicin encapsulation in poly N-isopropylacrylamide-co-acrylic acid (PNA) gel in combination with CNTs mediated photothermal therapy can be an effective strategy to inhibit tumor cells [83]. Doxycycline encapsulated in photothermal agent polydopamine (PDA) has been shown to be effective in the treatment of oral squamous cell carcinoma cell lines which may further be enhanced by conjugating with SWCNTs or MWCNTs [84].

Multi drug resistance (MDR) is a major problem due to use of a single drug and combination therapy serves as a promising approach to overcome the MDR. Delivery of CNTs with doxorubicin may reduce the chemoresistance in combination of photothermal therapy against drug resistant hepatocellular carcinoma in mouse [85]. Also, ribonuclease A (RNase A) conjugated gold nanoparticles are used in combination of photothermal therapy of colon cancer cells, which in turn may be synergistically enhanced in presence of CNTs [86]. CNTs-based photothermal therapy with immune-adjuvant nanoparticles together may attribute to checkpoint blockade for effective cancer immunotherapy [81]. Quantum dots based on black phosphorus in combination with CNTs-based photothermal therapy may effectively inhibit relapse and metastasis in triple-negative breast cancer (TNBC), which is one of the aggressive cancer types to treat and causes high mortality [87]. Likewise $CoFe_2O_4$-quantum dots functionalized on SWCNTS/MWCNTs may exhibit synergistic photothermal therapy in non-small-cell lung carcinoma due to induction of apoptosis by downregulating AKT signaling pathway [88–91]. Sonosensitizers such as, adriamycin, hematoporphyrin, ATX-70, pheophorbide A, ATXS10, and porfimer sodium, may act as sonosensitizer which can be functionalized on CNTs along with anticancer drugs with effective chemo-sono-photo-dynamic properties [92, 93].

Insolubility of CNTs in water is a key obstacle for gastrointestinal absorption, blood transportation, secretion, and biocompatibility and so on. Hence, dispersion can be ensured by developing strategies for wetting the hydrophobic tube surfaces and modifying the tube surfaces to decrease tube's bundle formation. Foldvari et al. have proposed four basic approaches for ensuring the uniform dispersion of CNTs in the aqueous medium which can be summarized as follows: (1) surfactant-assisted dispersion, (2) solvent dispersion, (3) functionalization of side walls, and (4) biomolecular dispersion. Among the above mentioned strategies, functionalization with hydrophilic moieties is considered as the most effective approach [94].

Cellular uptake of CNTs is a prerequisite for the therapeutic activity. Hence, proper distribution at the target sites and selective retention at the place of delivery are of great importance in clinical pharmacology of CNTs as drug carriers. PEG chain lengths is a key determining factor of the biodistribution and circulation of CNTs. PEG-5400-modified SWCNTs have a circulation time ($t_{1/2} = 2$ h) much longer than that of PEG-2000-modified counterpart ($t_{1/2} = 0.5$ h). Further, functionalization of the arginine-glycine-aspartic acid (RGD) peptide with the PEGylated SWCNTs facilitates the accumulation in integrin-positive U87MG tumors.

Moreover, adsorption of the shorter chain PEG (PL-PEG-2000) to CNTs cannot protect them from macrophagocytosis. However, adsorption of longer chain PEG (PL-PEG-5000) can effectively reduce nonspecific uptake of CNTs. It is important to note that functionalization of CNTs with PEG grafted branched polymers, namely poly(maleicanhydride-alt-1-octadecene)-PEG methyl ethers (PMHC18-mPEG) and poly (g-glutamic acid)-pyrine(30%)-PEG methylethers (70%) (gPGA-Py-mPEG), can enhance circulation time in the blood after intravenous injection [95].

The morphology of CNTs plays a crucial role in determining its drug loading capacity and delivery. The wall of CNTs results from rolling up of either single or multiple layers of graphene sheets forming SWCNTs or MWCNTs, respectively. Both SWCNTs and MWCNTs are capped at both ends of the tubes in a hemispherical arrangement of carbon networks called fullerenes warped up by the graphene sheet. Although the CNTs have various lengths from several hundreds of nanometers to several micrometers, they can be rationally shortened chemically or physically for their suitability for drug carriers. Opening both ends with useful wall defects facilitates intratube drug loading and chemical functionalization. Also, appropriate chemical treatment can result in development of desired charge on the surface of the nanotube that enable ionic interactions mediated adsorption of the charged molecules like drugs, targeting ligands and contrast agents. Aromatic molecules, nucleic acids and amphiphilic peptides can be functionalized based on the π-π stacking interactions between the CNT surface and aromatic bases/amino acids resulting in enhanced solubility and dispersion [95].

Another effective novel system developed by Li et al. is "dual-targeted drug nanocarrier" which was first reported by conjugating MWCNTs with iron nanoparticles and folate molecules [96]. Conjugation with targeted moieties of folate (FA) and an external magnetic field together facilitated the targeted delivery of doxorubicin into the HeLa cells. Similarly, FA-modified SWCNTs for targeted delivery of cisplatin into Ntera-2 cells, phosphatidylserine-modified SWCNTs for delivering cytochrome C into phagocytic cells, NPs-modified multiwall carbon nanotube (MWCNT) for delivering gemcitabine into lymph nodes and antibody-modified SWCNTs for delivering doxorubicin (Dox) into WiDr cells are examples for promising targeted delivery using CNTs. Such delivery systems can further be conjugated with magnetic probes for designing an effective dual targeting nanoplatform. This will ensure the delivery of anticancer drugs by guiding the nanocarriers to cancer sites efficiently using both receptor–ligand interaction and an external magnetic field.

Hence, several key factors should be considered before developing an ideal nanomedicine based on CNTs for effecting targeting and drag delivery in cancer.

## 5   Conclusions

Although, phototherapy alone has been effective against the cancer treatment since decades, Recent studies show promises for the CNTs mediated combination

therapy which can provide synergistic treatment modalities. Combination of CNTs-based phototherapy with chemotherapy may address the emerging chemoresistance among cancer cells. Similarly, combination of phototherapy with immunomodulatory inhibitors may provide great opportunities for synergistic personalized medicine. Immune checkpoint inhibitors and radiosensitizers combined with CNTs may offer novel combination to treat metastatic cancers. However, there is still a need for investigating the novel combinations of phototherapy with either chemotherapeutic agents or immunomodulatory inhibitors. Investigation of the most effective combination and performing further toxicological, pharmacokinetic and pharmacodynamic studies to confirm the efficacy and safety of CNTs-based nanomedicine for treatment and management of cancer would further help in establishing their therapeutic promises and safety.

**Conflict of Interest**   The authors declare that there are no conflicts of interest.

# References

1. Sung H, Ferlay J, Siegel RL, Laversanne M, Soerjomataram I, Jemal A, Bray F (2021) Global cancer statistics 2020: GLOBOCAN estimates of incidence and mortality worldwide for 36 cancers in 185 countries. CA Cancer J Clin 71(3):209–249
2. Iwamoto T (2013) Clinical application of drug delivery systems in cancer chemotherapy: review of the efficacy and side effects of approved drugs. Biol Pharm Bull 36(5):715–718
3. Hossein Z, Ahmadi S, Ghasemi A, Ghanbari M, Rabiee N, Bagherzadeh M, Karimi M, Webster TJ, Hamblin MR, Mostafavi E (2021) Carbon nanotubes: smart drug/gene delivery carriers. Int J Nanomedicine 16:1681–1706
4. Zarghami Dehaghani M, Yousefi F, Sajadi SM, Tajammal Munir M, Abida O, Habibzadeh S, Mashhadzadeh AH, Rabiee N, Mostafavi E, Saeb MR (2021) Theoretical encapsulation of fluorouracil (5-FU) anti-cancer chemotherapy drug into carbon nanotubes (CNT) and boron nitride nanotubes (BNNT). Molecules 26(16):4920
5. Mostafavi E, Soltantabar P, Webster TJ (2019) Nanotechnology and picotechnology: a new arena for translational medicine. In: Biomaterials in translational medicine. Academic Press, pp 191–212
6. Ghosh S, Harke AN, Chacko MJ, Gurav SP, Joshi KA, Dhepe A, Dewle A, Tomar GB, Kitture R, Parihar VS, Banerjee K, Kamble N, Bellare J, Chopade BA (2016) *Gloriosa superba* mediated synthesis of silver and gold nanoparticles for anticancer applications. J Nanomed Nanotechnol 7:4
7. Rokade S, Joshi K, Mahajan K, Patil S, Tomar G, Dubal D, Parihar VS, Kitture R, Bellare JR, Ghosh S (2018) *Gloriosa superba* mediated synthesis of platinum and palladium nanoparticles for induction of apoptosis in breast cancer. Bioinorg Chem Appl 2018:4924186
8. Rokade SS, Joshi KA, Mahajan K, Tomar G, Dubal DS, Parihar VS, Kitture R, Bellare J, Ghosh S (2017) Novel anticancer platinum and palladium nanoparticles from *Barleria prionitis*. Glob J Nanomedicine 2(5):555600
9. Ghosh S, Nitnavare R, Dewle A, Tomar GB, Chippalkatti R, More P, Kitture R, Kale S, Bellare J, Chopade BA (2015) Novel platinum-palladium bimetallic nanoparticles synthesized by *Dioscorea bulbifera*: anticancer and antioxidant activities. Int J Nanomedicine 10(1):7477–7490

10.  Ghosh S, More P, Derle A, Kitture R, Kale T, Gorain M, Avasthi A, Markad P, Kundu GC, Kale S, Dhavale DD, Bellare J, Chopade BA (2015) Diosgenin functionalized iron oxide nanoparticles as novel nanomaterial against breast cancer. J Nanosci Nanotechnol 15(12):9464–9472

11.  Ghosh S (2019) Mesoporous silica based nano drug delivery system synthesis, characterization and applications. In: Mohapatra SS, Ranjan S, Dasgupta N, Mishra RK, Thomas S (eds) Nanocarriers for drug delivery. Elsevier Inc. Amsterdam, pp 285–317. ISBN: 978-0-12-814033-8

12.  Kitture R, Ghosh S (2019) Hybrid nanostructures for in-vivo imaging. In: Bohara RA, Thorat N (eds) Hybrid nanostructures for cancer theranostics. Elsevier Inc. Amsterdam, pp 173–208, eBook ISBN: 9780128139073; Paperback ISBN:9780128139066

13.  Ghosh S, Patil PD, Kitture RD (2019) Physically responsive nanostructures in breast cancer theranostics. In: Thorat ND, Bauer J (eds) External field and radiation stimulated breast cancer nanotheranostics. IOP Publishing Ltd, United Kingdom, pp 2-1–2-24. Online ISBN: 978-0-7503-2416-8; Print ISBN: 978-0-7503-2414-4

14.  Dizaji BF, Khoshbakht S, Farboudi A, Azarbaijan MH, Irani M (2020) Far-reaching advances in the role of carbon nanotubes in cancer therapy. Life Sci 257:118059

15.  Liang X, Shang W, Chi C, Zeng C, Wang K, Fang C, Chen Q, Liu H, Fan Y, Tian J (2016) Dye-conjugated single-walled carbon nanotubes induce photothermal therapy under the guidance of near-infrared imaging. Cancer Lett 383(2):243–249

16.  Hernandez-Rivera M, Zaibaq NG, Wilson LJ (2016) Toward carbon nanotube-based imaging agents for the clinic. Biomaterials 101:229–240

17.  Lu GH, Shang WT, Deng H, Han ZY, Hu M, Liang XY, Fang CH, Zhu XH, Fan YF, Tian J (2019) Targeting carbon nanotubes based on IGF-1R for photothermal therapy of orthotopic pancreatic cancer guided by optical imaging. Biomaterials 195:13–22

18.  Nikfarjam M, Muralidharan V, Christophi C (2005) Mechanisms of focal heat destruction of liver tumors. J Surg Res 127:208–223

19.  He X (2011) Thermostability of biological systems: fundamentals, challenges, and quantification. Open Biomed Eng J 5:47–73

20.  Burke AR, Singh RN, Carroll DL, Wood JC, D'Agostino RB, Ajayan PM, Torti FM, Torti SV (2012) The resistance of breast cancer stem cells to conventional hyperthermia and their sensitivity to nanoparticle-mediated photothermal therapy. Biomaterials 33:2961–2970

21.  Singh R, Torti SV (2013) Carbon nanotubes in hyperthermia therapy. Adv Drug Deliv Rev 65:2045–2060

22.  Virani NA, Davis C, McKernan P, Hauser P, Hurst RE, Slaton J, Silvy RP, Resasco DE, Harrison RG (2018) Phosphatidylserine targeted single-walled carbon nanotubes for photothermal ablation of bladder cancer. Nanotechnology 29:035101

23.  Behnam MA, Emami F, Sobhani Z, Koohi-Hosseinabadi O, Dehghanian AR, Zebarjad SM, Moghim MH, Oryan A (2018) Novel combination of silver nanoparticles and carbon nanotubes for plasmonic photo thermal therapy in melanoma cancer model. Adv Pharm Bull 8(1):49–55

24.  Sobhani Z, Behnam MA, Emami F, Dehghanian A, Jamhiri I (2017) Photothermal therapy of melanoma tumor using multiwalled carbon nanotubes. Int J Nanomedicine 12:4509–4517

25.  Suo X, Eldridge BN, Zhang H, Mao C, Min Y, Sun Y, Singh R, Ming X (2018) P-glycoprotein-targeted photothermal therapy of drug-resistant cancer cells using antibody-conjugated carbon nanotubes. ACS Appl Mater Interfaces 10:33464–33473

26.  Dolmans DE, Fukumura D, Jain RK (2003) Photodynamic therapy for cancer. Nat Rev Cancer 3(5):380–387

27.  Fukuda R, Umeyama T, Tsujimoto M, Ishidate F, Tanaka T, Kataura H, Imahori H, Murakami T (2020) Sustained photodynamic effect of single chirality-enriched single walled carbon nanotubes. Carbon 161:718–725

28.  Ogbodu RO, Limson JL, Prinsloo E, Nyokong T (2015) Photophysical properties and photodynamic therapy effect of zinc phthalocyanine-spermine-single walled carbon nanotube conjugate on MCF-7 breast cancer cell line. Synth Met 204:122–132

29.  Ogbodu RO, Nyokong T (2015) The effect of ascorbic acid on the photophysical properties and photodynamic therapy activities of zinc phthalocyanine-single walled carbon nanotube conjugate on MCF-7 cancer cells. Spectrochim Acta A Mol Biomol Spectrosc 151:174–183

30. Sundaram P, Abrahamse H (2020) Effective photodynamic therapy for colon cancer cells using chlorin e6 coated hyaluronic acid-based carbon nanotubes. Int J Mol Sci 21:4745

31. Cheng J, Liang H, Li Q, Peng C, Li Z, Shi S, Yang L, Tian Z, Tian Y, Zhang Z, Cao W (2010) Hematoporphyrin monomethyl ether-mediated photodynamic effects on THP-1 cell-derived macrophages. J Photochem Photobiol B 101(1):9–15

32. Shi J, Ma R, Wang L, Zhang J, Liu R, Li L, Liu Y, Hou L, Yu X, Gao J, Zhang Z (2013) The application of hyaluronic acid-derivatized carbon nanotubes in hematoporphyrin monomethyl ether-based photodynamic therapy for in vivo and in vitro cancer treatment. Int J Nanomedicine 8:2361–2373

33. Wang H, Pan X, Wang X, Wang W, Huang Z, Gu K, Liu S, Zhang F, Shen H, Yuan Q, Ma J, Yuan W, Liu H (2020) Degradable carbon−silica nanocomposite with immunoadjuvant property for dual-modality photothermal/photodynamic therapy. ACS Nano 14:2847–2859

34. Zhang M, Wang W, Cui Y, Chu X, Sun B, Zhou N, Shen J (2018) Magnetofluorescent $Fe_3O_4$/carbon quantum dots coated single-walled carbon nanotubes as dual-modal targeted imaging and chemo/photodynamic/photothermal triple-modal therapeutic agents. Chem Eng J 338:526–538

35. Li H, Zhang N, Hao Y, Wang Y, Jia S, Zhang H (2019) Enhancement of curcumin antitumor efficacy and further photothermal ablation of tumor growth by single-walled carbon nanotubes delivery system in vivo. Drug Deliv 26(1):1017–1026

36. Yi W, Zhang P, Hou J, Chen W, Bai L, Yoo S, Khalid A, Hou X (2018) Enhanced response of tamoxifen toward the cancer cells using a combination of chemotherapy and photothermal abla-tion induced by lentinan-functionalized multi-walled carbon nanotubes. Int J Biol Macromol 120:1525–1532

37. Zhang P, Yi W, Hou J, Yoo S, Jin W, Yang Q (2018) A carbon nanotube-gemcitabine-lentinan three-component composite for chemo-photothermal synergistic therapy of cancer. Int J Nanomedicine 13:3069–3080

38. Yoo S, Hou J, Yi W, Li Y, Chen W, Meng L, Si J, Hou X (2017) Enhanced response of metformin towards the cancer cells due to synergism with multi-walled carbon nanotubes in photothermal therapy. Sci Rep 7:1071

39. Zhou F, Wu S, Song S, Chen WR, Resasco DE, Xing D (2012) Antitumor immunologically modified carbon nanotubes for photothermal therapy. Biomaterials 33(11):3235–3242

40. Wang C, Xu L, Liang C, Xiang J, Peng R, Liu Z (2014) Immunological responses triggered by photothermal therapy with carbon nanotubes in combination with anti-CTLA-4 therapy to inhibit cancer metastasis. Adv Mater 26(48):8154–8162

41. Kohshour MO, Mirzaie S, Zeinali M, Amin M, Hakhamaneshi MS, Jalili A, Mosaveri N, Jamalan M (2014) Ablation of breast cancer cells using trastuzumab-functionalized multi-walled carbon nanotubes and trastuzumab-diphtheria toxin conjugate. Chem Biol Drug Des 83:259–265

42. Behzadpour N, Ranjbar A, Azarpira N, Sattarahmady N (2020) Development of a composite of polypyrrole-coated carbon nanotubes as a sonosensitizer for treatment of melanoma cancer under multi-step ultrasound irradiation. Ultrasound Med Biol 46(9):2322–2334

43. Yumita N, Iwase Y, Umemura SI, Chen FS, Momose Y (2020) Sonodynamically-induced anti-cancer effects of polyethylene glycol-modified carbon nanotubes. Anticancer Res 40(5):2549–2557

44. Bosca F, Corazzari I, Foglietta F, Canaparo R, Durando G, Pastero L, Arpicco S, Dosio F, Zonari D, Cravotto G, Tagliapietra S (2020) SWCNT–porphyrin nano-hybrids selectively activated by ultrasound: an interesting model for sonodynamic applications. RSC Adv 10(37):21736–21744

45. Wang CJ, Li W (2016) Preparation and sonodynamic antitumor effect of protohemin-conjugated multiwalled carbon nanotubes functionalized with carboxylic group. Drug Dev Res 77:152–158

46. Wang CJ, Wang HZ, Li W (2019) A novel conjunction of folate-targeted carbon nanotubes containing protohemin and oridonin-liposome loaded microbubbles for cancer chemo-sonodynamic therapy. J Drug Target 27(10):1076–1083

47. Bhowmik A, Khan R, Ghosh MK (2015) Blood-brain barrier: a challenge for effectual therapy of brain tumors. Biomed Res Int 2015:320941. https://doi.org/10.1155/2015/320941
48. Omuro A, DeAngelis LM (2013) Glioblastoma and other malignant gliomas: a clinical review. JAMA 310(17):1842–1850
49. Salazar A, Cruz VP la, Muñoz-Sandoval E, Chavarria V, Morales M de LG, Espinosa-Bonilla A, Sotelo J, Jiménez-Anguiano A, Pineda B (2021) Potential use of nitrogen-doped carbon nanotube sponges as payload carriers against malignant glioma. Nanomaterials-basel 11(5):1244
50. Stupp R, Mason WP, van den Bent MJ, Weller M, Fisher B, Taphoorn MJB, Belanger K, Brandes AA, Marosi C, Bogdahn U, Curschmann J, Janzer RC, Ludwin SK, Gorlia T, Allgeier A, Lacombe D, Cairncross JG, Eisenhauer E, Mirimanoff RO (2005) Radiotherapy plus concomitant and adjuvant temozolomide for glioblastoma. New Engl J Med 352(10):987–996
51. Zhao D, Badie B (2007) Application of carbon nanotubes to brain tumor therapy. Nanotechnologies for the life sciences. Wiley-VCH Verlag GmbH & Co. KGaA, pp 381–402
52. Stupp R, Hegi ME, Mason WP, Bent MJ van den, Taphoorn MJB, Janzer RC, Ludwin SK, Allgeier A, Fisher B, Belanger K, Hau P, Brandes AA, Gijtenbeek J, Marosi C, Vecht CJ, Mokhtari K, Wesseling P, Villa S, Eisenhauer E, Gorlia T, Weller M, Lacombe D, Cairncross JG, Mirimanoff R-O, Groups EO for R and T of CBT and RO, Group NCI of CCT (2009) Effects of radiotherapy with concomitant and adjuvant temozolomide versus radiotherapy alone on survival in glioblastoma in a randomised phase III study: 5-year analysis of the EORTC-NCIC trial. Lancet Oncol 10(5):459–66
53. Alizadeh D, White EE, Sanchez TC, Liu S, Zhang L, Badie B, Berlin JM (2018) Immunostimulatory CpG on carbon nanotubes selectively inhibits migration of brain tumor cells. Bioconjugate Chem 29(5):1659–1668
54. Davis M (2016) Glioblastoma: overview of disease and treatment. Clin J Oncol Nurs 20(5):S2–S8
55. Wen PY, Reardon DA (2016) Progress in glioma diagnosis, classification and treatment. Nat Rev Neurol 12(2):69–70
56. Gheith MK, Pappas TC, Liopo AV, Sinani VA, Shim BS, Motamedi M, Wicksted JP, Kotov NA (2006) Stimulation of neural cells by lateral currents in conductive layer-by-layer films of single-walled carbon nanotubes. Adv Mater 18(22):2975–2979. https://doi.org/10.1002/adma.200600878
57. Singh R, Pantarotto D, Lacerda L, Pastorin G, Klumpp C, Prato M, Bianco A, Kostarelos K (2006) Tissue biodistribution and blood clearance rates of intravenously administered carbon nanotube radiotracers. Proc National Acad Sci 103(9):3357–3362
58. Kievit FM, Zhang M (2011) Cancer therapy: cancer nanotheranostics: improving imaging and therapy by targeted delivery across biological barriers. Adv Mater 23(36):H209–H209
59. Klinman DM (2004) Immunotherapeutic uses of CpG oligodeoxynucleotides. Nat Rev Immunol 4(4):249–259. https://doi.org/10.1038/nri1329
60. Jahrsdörfer B, Weiner GJ (2008) CpG oligodeoxynucleotides as immunotherapy in cancer. Updat Cancer Ther 3(1):27–32
61. Zhao D, Alizadeh D, Zhang L, Liu W, Farrukh O, Manuel E, Diamond DJ, Badie B (2010) Carbon nanotubes enhance CpG uptake and potentiate antiglioma immunity. Clin Cancer Res 17(4):771–782
62. Ouyang M, White EE, Ren H, Guo Q, Zhang I, Gao H, Yanyan S, Chen X, Weng Y, Fonseca AD, Shah S, Manuel ER, Zhang L, Vonderfecht SL, Alizadeh D, Berlin JM, Badie B (2016) Metronomic doses of temozolomide enhance the efficacy of carbon nanotube CpG immunotherapy in an invasive glioma model. PLoS ONE 11(2):e0148139
63. You Y, Wang N, He L, Shi C, Zhang D, Liu Y, Luo L, Chen T (2018) Designing dual-functionalized carbon nanotubes with high blood-brain-barrier permeability for precise orthotopic glioma therapy. Dalton Transactions Camb Engl 48(5):1569–1573
64. Daneman R, Prat A (2015) The blood-brain barrier. Csh Perspect Biol 7(1):a020412
65. Kafa H, Wang JT-W, Rubio N, Venner K, Anderson G, Pach E, Ballesteros B, Preston JE, Abbott NJ, Al-Jamal KT (2015) The interaction of carbon nanotubes with an in vitro blood-brain barrier model and mouse brain in vivo. Biomaterials 53:437–452

66. Zhao X, Shang T, Zhang X, Ye T, Wang D, Rei L (2016) Passage of magnetic tat-conjugated $Fe_3O_4@SiO_2$ nanoparticles across in vitro blood-brain barrier. Nanoscale Res Lett 11(1):451

67. Gump JM, Dowdy SF (2007) TAT transduction: the molecular mechanism and therapeutic prospects. Trends Mol Med 13(10):443–448

68. Kaliki S, Shields CL (2015) Retinoblastoma: achieving new standards with methods of chemotherapy. Indian J Ophthalmol 63(2):103–109

69. Young JL, Smith MA, Roffers SD, Liff JM, Bunin GR (2012) Retinoblastoma. In: Ries LA, Smith MA, Gurney JG, Linet M, Tamra T, Young JL et al (eds) Cancer incidence and survival among children and adolescents: United States SEER program 1975–1995. National Cancer Institute, Maryland, SEER Program

70. Murphy D, Bishop H, Edgar A (2012) Leukocoria and retinoblastoma—pitfalls of the digital age? Lancet Lond Engl 379(9835):2465

71. Kansara V, Luo S, Balasubrahmanyam B, Pal D, Mitra AK (2006) Biotin uptake and cellular translocation in human derived retinoblastoma cell line (Y-79): a role of hSMVT system. Int J Pharmaceut 312(1–2):43–52

72. Kansara V, Paturi D, Luo S, Gaudana R, Mitra AK (2007) Folic acid transport via high affinity carrier-mediated system in human retinoblastoma cells. Int J Pharmaceut 355(1–2):210–219

73. Jwala J, Vadlapatla RK, Vadlapudi AD, Boddu SHS, Pal D, Mitra AK (2012) Differential expression of folate receptor-alpha, sodium-dependent multivitamin transporter, and amino acid transporter (B(0, +)) in human retinoblastoma (Y-79) and retinal pigment epithelial (ARPE-19) cell lines. J Assoc Ocular Pharmacol Ther 28(3):237–244

74. Demirci H, Wang Y, Li Q, Lin C-M, Kotov NA, Grisolia ABD, Guo JL (2020) Penetration of carbon nanotubes into the retinoblastoma tumor after intravitreal injection in $LH_{BETA}T_{AG}$ transgenic mice reti-noblastoma model. J Ophthalmic Vis Res 15(4):446–452

75. Browning RJ, Able S, Ruan JL, Bau L, Allen PD, Kersemans V, Wallington S, Kinchesh P, Smart S, Kartsonaki C, Kamila S, Logan K, Taylor MA, McHale AP, Callan JF, Stride E, Vallis KA (2021) Combining sonodynamic therapy with chemoradiation for the treatment of pancreatic cancer. J Control Release 337:371–377

76. Yuan H, Fales AM, Vo-Dinh T (2012) TAT peptide-functionalized gold nanostars: enhanced intracellular delivery and efficient NIR photothermal therapy using ultralow irradiance. J Am Chem Soc 134(28):11358–11361

77. Nam J, Son S, Ochyl LJ, Kuai R, Schwendeman A, Moon JJ (2018) Chemo-photothermal therapy combination elicits anti-tumor immunity against advanced metastatic cancer. Nat Commun 9(1):1074

78. Lee C, Hwang HS, Lee S, Kim B, Kim JO, Oh KT, Lee ES, Choi HG, Youn YS (2017) Rabies virus-inspired silica-coated gold nanorods as a photothermal therapeutic platform for treating brain tumors. Adv Mater 29(13). https://doi.org/10.1002/adma.201605563

79. Yu G, Yang Z, Fu X, Yung BC, Yang J, Mao Z, Shao L, Hua B, Liu Y, Zhang F, Fan Q, Wang S, Jacobson O, Jin A, Gao C, Tang X, Huang F, Chen X (2018) Polyrotaxane-based supramolecular theranostics. Nat Commun 9:766

80. Guo B, Sheng Z, Hu D, Liu C, Zheng H, Liu B (2018) Through scalp and skull NIR-II photothermal therapy of deep orthotopic brain tumors with precise photoacoustic imaging guidance. Adv Mater 30(35):1802591

81. Chen Q, Xu L, Liang C, Wang C, Peng R, Liu Z (2016) Photothermal therapy with immune-adjuvant nanoparticles together with checkpoint blockade for effective cancer immunotherapy. Nature Commun 7:13193

82. Bai H, Sun Q, Kong F, Dong H, Ma M, Liu F, Wang C, Xu H, Gu N, Zhang Y (2021) Zwitterion-functionalized hollow mesoporous Prussian blue nanoparticles for targeted and synergetic chemo-photothermal treatment of acute myeloid leukemia. J Mater Chem B 9:5245–5254

83. Pu XQ, Ju XJ, Zhang L, Cai QW, Liu YQ, Peng HY, Xie R, Wang W, Liu Z, Chu LY (2021) Novel multifunctional stimuli-responsive nanoparticles for synergetic chemo-photothermal therapy of tumors. ACS Appl Mater Interfaces 13:28802–28817

84. Gu M, Jiang L, Hao L, Lu J, Liu Z, Lei Z, Li Y, Hua C, Li W, Li X (2021) A novel thera-nostic nanoplatform for imaging-guided chemo-photothermal therapy in oral squamous cell carcinoma. J Mater Chem B 9(30):6006–6016

85. Du Z, Mao Y, Zhang P, Hu J, Fu J, You Q, Yin J (2021) TPGS-galactose-modified poly-dopamine co-delivery nanoparticles of nitric oxide donor and doxorubicin for targeted chemo-photothermal therapy against drug-resistant hepatocellular carcinoma. ACS Appl Mater Interfaces 13(30):35518–35532

86. Goodrich GP, Bao L, Gill-Sharp K, Sang KL, Wang J, Payne JD (2010) Photothermal therapy in a murine colon cancer model using near-infrared absorbing gold nanorods. J Biomed Opt 15:018001

87. Zhao P, Xu Y, Ji W, Zhou S, Li L, Qiu L, Qian Z, Wang X, Zhang H (2021) Biomimetic black phosphorus quantum dots-based photothermal therapy combined with anti-PD-L1 treatment inhibits recurrence and metastasis in triple-negative breast cancer. J Nanobiotechnology 19(1):181

88. Xia QH, Lu CT, Tong MQ, Yue M, Chen R, Zhuge DL, Yao Q, Xu HL, Zhao YZ (2021) Ganoderma lucidum polysaccharides enhance the abscopal effect of photothermal therapy in hepatoma-bearing mice through immunomodulatory, anti-proliferative, pro-apoptotic and anti-angiogenic. Front Pharmacol 12:648708

89. Odion RA, Liu Y, Vo-Dinh T (2021) Plasmonic gold nanostar-mediated photothermal immunotherapy. IEEE J Sel Top Quantum Electron 27(5):4800109

90. Liu Y, Chongsathidkiet P, Crawford BM, Odion R, Dechant CA, Kemeny HR, Cui X, Maccarini PF, Lascola CD, Fecci PE, Vo-Dinh T (2019) Plasmonic gold nanostar-mediated photothermal immunotherapy for brain tumor ablation and immunologic memory. Immunotherapy 11(15):1293–1302

91. Kremkau FW (1979) Cancer therapy with ultrasound: a historical review. J Clin Ultrasound 7:287–300

92. Umemura K, Yumita N, Nishigaki R, Umemura S (1996) Sonodynamically induced antitumor effect of pheophorbide a. Cancer Lett 102:151–157

93. Jin ZH, Miyoshi N, Ishiguro K, Umemura S, Kawabata K, Yumita N, Sakata I, Takaoka K, Udagawa T, Nakajima S, Tajiri H, Ueda K, Fukuda M, Kumakiri M (2000) Combination effect of photodynamic and sonodynamic therapy on experimental skin squamous cell carcinoma in $C_3H/HeN$ mice. J Dermatol 27:294–306

94. Foldvari M, Bagonluri M (2008) Carbon nanotubes as functional excipients for nanomedicines: I pharmaceutical properties. Nanomedicine 3:173–182

95. Zhang W, Zhang Z, Zhang Y (2011) The application of carbon nanotubes in target drug delivery systems for cancer therapies. Nanoscale Res Lett 6:555

96. Li R, Wu R, Zhao L, Hu Z, Guo S, Pan X, Zou H (2011) Folate and iron difunctional-ized multiwall carbon nanotubes as dual-targeted drug nanocarrier to cancer cells. Carbon 49(5):1797–1805